ADVANCES IN ATMOSPHERIC SCIENCES, VOL. 26, NO. 1, 2009, 180–190

The Characteristics and Parameterization of Aerodynamic Roughness Length over Heterogeneous Surfaces

LU Li[1,2] (卢 俐), LIU Shaomin*[1] (刘绍民), XU Ziwei[1] (徐自为), YANG Kun[3] (阳 坤), CAI Xuhui[4] (蔡旭辉), JIA Li[5] (贾 立), and WANG Jiemin[6] (王介民)

[1]*State key Laboratory of Remote Sensing Science, School of Geography, Beijing Normal University, Beijing* 100875

[2]*Meteorological Information Center of Beijing, Beijing Meteorological Bureau, Beijing* 100089

[3]*Institute of Tibetan Plateau Research, Chinese Academy of Sciences, Beijing* 100085

[4]*Department of Environment Science, Peking University, Beijing* 100871

[5]*Alterra Green World Research Institute, Wageningen University and Research Centre, Wageningen, The Netherlands*

[6]*Cold and Arid Regions Environment and Engineering Research Institute, Chinese Academy of Sciences, Lanzhou* 730000

(Received 30 November 2007; revised 27 July 2008)

ABSTRACT

Aerodynamic roughness length ($z_{0\mathrm{m}}$) is a key factor in surface flux estimations with remote sensing algorithms and/or land surface models. This paper calculates $z_{0\mathrm{m}}$ over several land surfaces, with 3 years of experimental data from Xiaotangshan. The results show that $z_{0\mathrm{m}}$ is direction-dependent, mainly due to the heterogeneity of the size and spatial distribution of the roughness elements inside the source area along different wind directions. Furthermore, a heuristic parameterization of the aerodynamic roughness length for heterogeneous surfaces is proposed. Individual $z_{0\mathrm{m}}$ over each surface component (patch) is calculated firstly with the characteristic parameters of the roughness elements (vegetation height, leaf area index, etc.), then $z_{0\mathrm{m}}$ over the whole experimental field is aggregated, using the footprint weighting method.

Key words: aerodynamic roughness length, heterogeneous surfaces, footprint

Citation: Lu, L., S. M. Liu, Z. W. Xu, K. Yang, X. H. Cai, L. Jia, and J. M. Wang, 2009: The characteristics and parameterization of aerodynamic roughness length over heterogeneous surfaces. *Adv. Atmos. Sci.*, **26**(1), 180–190, doi: 10.1007/s00376-009-0180-3.

1. Introduction

Aerodynamic roughness length ($z_{0\mathrm{m}}$) is a key parameter to describe the aerodynamic characteristics of land surfaces (Liu et al., 2007a). It is also an important parameter in determining mass and energy exchanges between the land surface and the atmosphere. Originally, $z_{0\mathrm{m}}$ is defined as the height where the wind speed, given by the extrapolation of the logarithmic wind profile, becomes zero. According to numerous observations, the variation range of $z_{0\mathrm{m}}$ over different surfaces is large, from an order of 1.0 m over urban areas and mountainous areas, to an order of 0.1 mm or even 0.01 mm over smooth water body surfaces, ice and snow surfaces (Sheng et al., 2003). Brutsaert (1982) gave a review: $z_{0\mathrm{m}}$ is 0.00001 m over ice sur-

*Corresponding author: LIU Shaomin, smliu@bnu.edu.cn

faces, 0.4–1.65 m over forest and urban areas, and in between those values for grassland and sparse vegetation areas.

The traditional way to calculate z_{0m} is based on the Monin-Obukhov Similarity Theory, using wind profile measurements. The simple case is to extrapolate wind profile observations at several levels under neutral conditions to obtain z_{0m}. Under non-neutral conditions, it is necessary to solve the wind profile relationship iteratively to obtain a fitted solution. Furthermore, z_{0m} can also be obtained with an eddy covariance system observation at a single level. In practical applications, especially for remote sensing models and land surface models, it is difficult to obtain z_{0m} for a local or regional scale based only on station observations. Former researchers (Brutsaert, 1982; Waters et al., 2002) have proposed some parameterizations between the aerodynamic roughness length and the land surface properties [e.g., vegetation height, leaf area index (LAI), etc], since wind turbulence is controlled by the structure and spacing of roughness elements (plants and other obstacles) on the land surface, and z_{0m} describes the roughness characteristics of a surface (Garratt, 1992). These empirical relationships have been widely used. The most commonly used relationship is to assume z_{0m} proportional to the roughness element height (h). Large variations in the ratio of z_{0m}/h over different land surfaces have been found in the literature. For example, z_{0m}/h is 0.04 for sparse sorghum (Azevedo and Verma, 1986); 0.14 for small cotton (Kustas et al., 1989), and 0.8 for cotton of intermediate foliage density (Hatfield, 1989). Mathias et al., 1990) and Garratt (1992) reported $z_{0m}/h = 0.1$ as a rough estimate from a review of literature although Garratt noted that the ratio can range from 0.02 to 0.2 for natural surfaces based on an extensive review of the literature. In many land surface models, such as BATS (Biosphere-Atmosphere Transfer Scheme) and SiB (Simple Biosphere model), z_{0m} is taken as a constant according to vegetation type (Dorman and Sellers, 1989; Dickinson et al., 1993). In the CLM (Common Land Model) (Dai et al., 2003), z_{0m} is taken as a constant ratio of vegetation height, i.e., $z_{0m} = 0.07h$. In the remote sensing models used to estimate the regional evapotranspiration, for instance, the SEBS (the Surface Energy Balance System) uses the Normalized Difference Vegetation Index (NDVI) to determine z_{0m} (Jia et al., 2003), while the SEBAL (Surface Energy Balance Algorithms for Land) uses an empirical relationship with NDVI and albedo. (Waters et al., 2002). This parameterization was also used by Liu et al. (2007b) to calculate the regional evapotranspiration over heterogeneous surfaces with TM/ETM+ data.

Based on the data of the Xiaotangshan Experiment (Changping District of Beijing, China), which was conducted in 2002, 2004, and 2005 respectively, the objectives of this paper are: (1) to calculate z_{0m} over different surfaces and analyze the directional characteristics of z_{0m} over heterogeneous surfaces using an analytical footprint model; (2) to relate the estimated z_{0m} over heterogeneous surfaces to roughness element characteristic factors, and present a heuristic parameterization of z_{0m} as a reference for model parameterizations.

2. Description of experimental site and data

This experiment was carried out at the Xiaotangshan Experimental Station for Precision Agriculture (40°10′41″N, 116°26′52″E, 35 m above sea level) in Beijing. The experimental field was flat and open, 1000 m long from north to south and 500 m wide from east to west, divided into two equal smaller subplots (southern and northern, denoted as XTS_S and XTS_N, respectively) by an east-west oriented path. The fetch in the prevailing wind direction is sufficient to ensure the Monin-Obukhov similarity theory to be held. The general situations of the experiments in 2002, 2004, and 2005 are as follows.

The observation period in 2002 was from 26 March to 23 April and the land cover was bare soil. In 2002, the instruments were mounted in the center of the experimental field.

In 2004, the experiment was carried out from 30 May to 7 July. In the southern sub-plot field, the land cover was bare soil between 30 May and 11 June, while the maize plants started emerging around 12 June. The average vegetation height was 0.41 m at the end of the experiment. In the northern sub-plot, the field was covered by weeds with an average height of 0.26 m until it was plowed into bare soil on 15 June. Two sets of eddy covariance systems and automatic weather stations were installed in the center of the southern and northern sub-plot fields, respectively, to measure the surface fluxes and other meteorological variables.

In 2005, the experiment was from 1 May to 10 June and the experimental layout was almost the same as that in 2004. The southern sub-plot field was bare soil with maize seeding in the soil. The northern sub-plot field was inhabited by weeds with an average vegetation height of 0.12 m.

All the measurements were averaged every 10 minutes. The description of the sites and measurements used in this study are summarized in Tables 1 and 2.

To ensure the data quality, only the data that met the following criteria were selected for further analysis: (1) wind speed $u > 1.0$ m s^{-1}; (2) friction velocity $u_* > 0.01$ m s^{-1} (for a bare soil surface) or $u_* >$

Table 1. Site description.

Site	Date	Latitude/Longitude	Land cover/use	Mean vegetation height h (cm)
XTS	28 March–23 April 2002	40°10′1″N, 116°26′1″E	Bare soil	0
XTS_S	30 May–11 June 2004	40°10′41″N, 116°26′52″E	Bare soil	0
	12–24 June 2004		Maize (emerging)	17
	25 June–7 July 2004		Maize	41
XTS_N	30 May–15 June 2004	40°10′57″N, 116°26′54″E	Weed habitat	26
	16 June–7 July 2004		Bare soil	0
XTS_S	1 May–10 June 2005	40°10′41″N, 116°26′53″E	Bare soil	0
XTS_N	1 May–10 June 2005	40°10′55″N, 116°26′53″E	Weed habitat	12

XTS: Xiaotangshan; S: southern sub-plot; N: northern sub-plot.

Table 2. Measurements and instruments used in this study.

Variables	Instruments	Instrument height (m)	Observation site
Friction velocity u_*, Wind speed u, Monin-Obukhov length L	a 3D sonic anemometer (DA600, KAIJO, Japan) and a CO_2/H_2O analyzer (Li7500, Campbell).	2	XTS2002
	a 3D sonic anemometer (CSAT3, Campbell) and a CO_2/H_2O analyzer (Li7500, Campbell).	1.8	XTS2004_S
		1.9	XTS2004_N
		1.9	XTS2005_S
		2.0	XTS2005_N

0.1 m s^{-1} (for other surfaces); (3) sensible heat flux $H > 10$ W m^{-2}; (4) no rainfall; (5) measurements done between 0700 LST and 1800 LST.

3. Methods

3.1 *Aerodynamic roughness length* z_{0m}

With the development of eddy covariance techniques, mean wind speed and simultaneous measurements of turbulent fluxes measured at a single level by the sonic anemo-thermometer can be used to calculate $z_{0\mathrm{m}}$ (Chen et al., 1993; Jennifer and Brusaert, 1998; Jia and Wang, 1999; Martano, 2000). Yang et al. (2003) suggested an algorithm to obtain $z_{0\mathrm{m}}$ by minimizing the cost function below if the number of observations (i) was large enough:

$$J = \sum_i \{u_{*_i} - \kappa u_i/[\ln((z-d)/z_{0\mathrm{m}}) - \psi_{\mathrm{m}}(z_{0\mathrm{m}}/L_i, z/L_i)]\}^2 \, . \quad (1)$$

The Monin-Obukhov length L is obtained by using:

$$L = -\rho c_p u_*^3 T_{\mathrm{a}}/(\kappa g H) \, , \quad (2)$$

where u is the wind speed at observation level z, u_* is the friction velocity, and κ is the von Karman constant (0.4). The zero-plane displacement d is taken empirically, $d = 2/3h$ (Brutsaert, 1982). ρ is air density, c_p is the specific heat of air at constant pressure, T_{a} is the air temperature, g is the gravitational acceleration (9.81 m s^{-2}), and H is the sensible heat flux. Under unstable conditions, the stability correction function for the momentum transfer ψ_m is expressed as (Paulson, 1970):

$$\psi_m = 2\ln\left[\frac{(1+x)}{2}\right] + \ln\left[\frac{(1+x^2)}{2}\right] - 2\arctan x + \frac{\pi}{2} \, . \quad (3)$$

Under stable conditions (Webb, 1970; Businger et al., 1971):

$$\psi_m = -5\xi \, , \quad (4)$$

where

$$\xi = (z-d)/L \, , \quad (5)$$

$$x = (1-16\xi)^{1/4} \, . \quad (6)$$

The selected data set was divided into four subsets according to the wind direction (dir): East (E in short, 45° < dir ⩽ 135°), South (S in short, 135° < dir ⩽ 225°), West (W in short, 225° < dir ⩽ 315°), North (N in short, 315° < dir ⩽ 360° and 0° < dir ⩽ 45°) and the z_{0m} of the four wind directions ($z_{0\mathrm{m\_E}}, z_{0\mathrm{m\_S}}, z_{0\mathrm{m\_W}}, z_{0\mathrm{m\_N}}$) were calculated using Eq. (1) (Table 3). Then, the four sub-set data were joined together to calculate another $z_{0\mathrm{m}}$ that can be deemed

Table 3. The z_{0m} obtained from the eddy covariance system observations (units: cm) (Xiaotangshan Experiment, 2002, 2004 and 2005).

	Date & site	Land cover/use	$z_{\mathrm{0m\_E}}$	$z_{\mathrm{0m\_S}}$	$z_{\mathrm{0m\_W}}$	$z_{\mathrm{0m\_N}}$	z_{0m}
2002	28 March–23 April, XTS	Bare soil	1.00	1.00	1.00	1.00	1.00
2004	30 May–11 June, XTS_S	Bare soil	0.74	0.95	0.13	0.13	0.58
	12–24 June, XTS_S	Maize (emerging)	1.87	2.37	1.85	0.65	1.86
	25 June–7 July, XTS_S	Maize field	3.94	4.30	1.70	1.34	2.59
	30 May–15 June, XTS_N	Weed habitat	2.70	2.76	0.44	1.03	2.25
	16 June–7 July, XTS_N	Bare soil	2.24	3.45	1.13	1.41	2.24
2005	1–10 May, XTS_S	Bare soil	0.71	0.56	0.57	0.09	0.56
	11–20 May, XTS_S		1.28	0.68	0.27	0.16	0.60
	21–31 May, XTS_S		1.64	1.15	0.39	0.24	0.80
	1–10 June, XTS_S		1.26	0.85	0.77	0.42	0.73
	1–10 May, XTS_N	Weed habitat	1.62	1.66	0.84	0.20	1.25
	11–20 May, XTS_N		1.78	1.95	0.85	0.41	1.41
	21–31 May, XTS_N		1.88	1.95	0.95	0.71	1.50
	1–10 June, XTS_N		1.56	0.69	1.45	0.86	1.00

as a representative of the roughness characteristics of the whole experimental field. It is listed on the last column of Table 3.

3.2 *Footprint model*

A footprint is specified as the relative contribution from each element of the upwind surface source area to the measured concentration or vertical flux (Schuepp et al., 1990). It describes the area of influence to a measurement, and is also called the source weight function. Source area is the area bounded by a source weight function isopleth and it is a region in the upwind direction of the location of the observation instrument (Schmid, 2002). The concept of the footprint provides a quantitative tool to establish the spatial frame of reference of surface-atmosphere exchange measurements. It may be interpreted in analogy to the "field of view" of the instrument. In this study, an analytical model is used to compute the flux footprint or upwind source area contributing to the measurements by the eddy covariance system. The footprint or source weight function is expressed as (Kormann and Meixner, 2001; Cai and Leclerc, 2007):

$$f_{\mathrm{t}}=\frac{1}{\Gamma(\mu)}\frac{\zeta^{\mu}}{x_1^{1+\mu}}e^{-\zeta/x_1} \qquad (7)$$

where f_{t} is the crosswind integrated flux footprint, μ is a constant, Γ is the Gamma function, and x_1 is the upwind distance from the point where the measurements are taken. ζ is the flux length scale and $\zeta=(Uz_1^r)/(r^2K)$, in which U is the constant in the assumed power-law profile of the wind velocity, z_1 is the height in the vertical direction, r is the shape factor, and K is the constant in the assumed power-law profile of the eddy diffusivity. For more information, please refer to Kormann and Meixner (2001).

4. Results and analysis

4.1 *The aerodynamic roughness length* (z_{0m}) *at the Xiaotangshan experimental fields*

Since z_{0m} is mainly related to the underlying surface, we can assume that z_{0m} is constant over short periods for a specific land surface condition. Table 3 shows the results of z_{0m} for the four wind direction classes described above and that of the whole experimental field in 2002, 2004, and 2005 respectively. The z_{0m} in 2004 and 2005 were calculated about every 10 days. The table shows: (1) the z_{0m} is in an order of 0.1–1 cm; (2) over a vegetation surface, z_{0m} increases during the crop-growing period in the summer because the form-drag around the surface roughness elements was enhanced; (3) at the northern sub-plot field in 2004, z_{0m} has a small variation before and after the weeds were cut, which means that the drag exerted by the permeable and the rougher vegetation surface (with average height 0.26 m) was about the same as the impermeable and uneven plowed surface; (4) the value of z_{0m} obviously varied with the types of bare soil surfaces, due to different morphology. Therefore, z_{0m} is mainly determined by the size, height, and layout of the surface roughness elements.

In the same sub-period, values of $z_{\mathrm{0m\_E}}$, $z_{\mathrm{0m\_S}}$, $z_{\mathrm{0m\_W}}$, and $z_{\mathrm{0m\_N}}$ showed a large variation (except in 2002 when the experimental field was smooth and flat bare soil). Over the heterogeneous surfaces, aerodynamic roughness length has directional characteristics. Here, taken the northern sub-plot in 2005 as an example, we use the analytical footprint model introduced in section 3.2 to explain this directional dependence.

During the first three periods of 2005, the maximum aerodynamic roughness length appeared in the southern direction, while the minimum was in the nor-

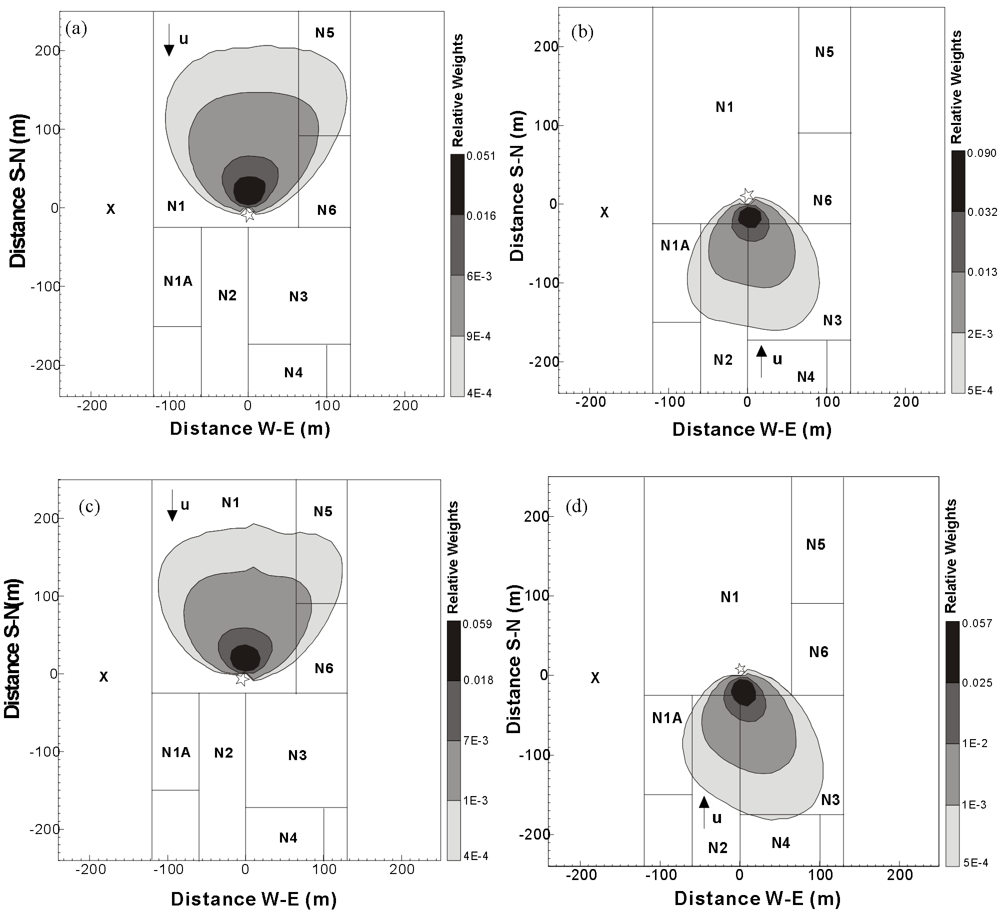

Fig. 1. The footprint of the eddy covariance system at northerly and southerly wind directions of the Xiaotangshan Experiment (northern sub-plot) overlays on the land cover map. Arrows denote wind direction. Stars denote the location of the apparatus with a coordinate of (0, 0). The longest isopleth determines the source area of a 90% level that limits an area that contributes up to 90% of the sensed fluxes by the instrumentation. (a, b: 1–31 May 2005; c, d: 1–10 June 2005).

thern direction (Table 3). Figure 1 shows the source area of the eddy covariance system measurement, overlying on the land cover map, along the northerly and southerly wind directions from 1–31 May (Figs. 1a, 1b) and 1–10 June (Figs. 1c, 1d). It clearly shows that the source area, both in the southerly and northerly wind directions, fell in the northern sub-plot field completely. The dimensions were about 150×150 m^2 (1–31 May), 180×180 m^2 (1–10 June) for the southerly wind direction and 200×200 m^2 (1–10 June) for the northerly wind direction, respectively. The source area for the northerly wind direction is almost in the N1 plot (morning glory field), except for a small part in the N5 plot (seedling) and the N6 plot (barren) that is at the edge of the source area and has little impact on the eddy covariance system measurement. For the southerly wind direction, most of the source areas are in the N2 (seedling) and N3 (barren) plots. The vegetation height of each plot is listed in Table 4. The vegetation height in plots N2 and N3 was much higher than that in N1, so aerodynamic roughness length in the southerly wind direction ($z_{0\mathrm{m\_S}}$) is larger than that in the northerly wind direction ($z_{0\mathrm{m\_N}}$). But a sharp decrease of $z_{0\mathrm{m\_S}}$ was found during 1–10 June and it became the minimum among the four directions. This is because during 1–10 June most of the source area of the southerly wind direction fell in the N3 plot (Fig. 1d) because the vegetation was harvested on 25 May and the land surface became bare soil (Table 4). Consequently, the $z_{0\mathrm{m}}$ in this period decreases significantly (Table 3). Thus, the essence of directional dependence is that the aerodynamic roughness length varies with the variation of terrain relief and roughness elements in the source areas of the measurements. Over heterogeneous surfaces, the size and spatial distribution of roughness elements within the source areas are different in different wind directions; the values of aerodynamic roughness length vary accordingly.

4.2 *The relationship between aerodynamic roughness length over heterogeneous surfaces and roughness elements in the source area*

The concept of the aerodynamic roughness length is straightforward in the case of homogeneous surface conditions. However, if one deals with the phenomena over heterogeneous surfaces with various types of vegetation, buildings, and possibly topography changes, the meaning of aerodynamic roughness length becomes less obvious. In such cases, the $z_{0\mathrm{m}}$ can be probably best defined as the parameter that should yield the correct surface stress over the area (Marshall, 1971; Mason, 1988; Menenti and Ritchie, 1994; Hiyama et al., 1996). Some researchers defined this as the "effective roughness length" (Fiedler and Panofsky, 1972; Wieringa, 1986; Mason, 1988). This means that the $z_{0\mathrm{m}}$ over heterogeneous surfaces (effective $z_{0\mathrm{m}}$) is not necessarily equal to the average of the roughness length values of all individual surface components. The form drag caused by isolated houses, trees, or sharp edges of forest/grassland, are not accounted for in an individual local roughness parameter, while they are major contributors to the areal surface stresses.

In practical use, especially for remote sensing and land surface models with pixel or grid resolution, it is difficult to obtain $z_{0\mathrm{m}}$ over heterogeneous surfaces via observation. Alternatively, indirect approaches have also been considered in previous studies as mentioned above.

In the following study, we try to find the relationship between the aerodynamic roughness length over heterogeneous surfaces and roughness elements in the source area based on the Xiaotangshan observations, and propose a heuristic parameterization of the aerodynamic roughness length over heterogeneous surfaces as a reference for model parameterizations.

During the three observation periods, the experimental surfaces were variable because of vegetation growth or field plowing. According to the study objectives, the surface conditions, and data availability, we chose two typical surfaces consisting of different patches: (1) 25 June–7 July 2004, the southern subplot field (Area A hereafter); (2) 21–31 May 2005, the northern sub-plot field (Area B hereafter). Figure 2 is the corresponding land cover map. The two heterogeneous surfaces were all consisting of bare soil patches and vegetation patches, and the latter one was the main type. All of the vegetation patches have two characteristics: (1) sparse vegetation ($0 \leqslant \mathrm{LAI} \leqslant 1$); (2) the vegetation height was obviously different for different patches because of different crop growing periods and/or vegetation types (Tables 4, 5). Therefore, we tried to analyze the relationship between the aerodynamic roughness length over heterogeneous surfaces and three key vegetation parameters which can describe the geometry and distribution of the surface roughnesses (vegetation height, fractional vegetation cover (f_{v}), and LAI). In this study, the last two parameters were derived from TM image data by assuming f_{v} and LAI as constant during the corresponding sub-periods [the satellite pass time: 6 July 2004 (Area A); 22 May 2005 (Area B)]. The vegetation height was measured and listed in Tables 4 and 5.

Among the available models in estimating the aerodynamic roughness length based on surface features, there was one proposed by Choudhury and Monteith (1988) who fitted simple functions to the curves obtained by Shaw and Pereira (1982) from second-order closure theory. For sparse vegetation ($0 \leqslant \mathrm{LAI} \leqslant 1$) like our experimental field:

$$z_{0\mathrm{m}} = z_0' + 0.3h(C_{\mathrm{d}} \times \mathrm{LAI})^{1/2}\ , \tag{8}$$

where h is the vegetation height, C_{d} is the mean drag coefficient for individual leaves assumed to be uniform within the canopy, and z_0' is the roughness length of the substrate and assigned to be 1 cm in our cases, according to Table 3. The main interest of this formulation, compared with the parameterization of a function of height, is to take into account an additional parameter (LAI) and thus be more suited to sparse vegetation when vegetation height remains constant

Table 4. Vegetation height measurement at the northern sub-plot field of the Xiaotangshan Experiment in 2005 (units: cm).

Plot	12 May	24 May	25 May	28 May
N1 (morning glory field)	11	13	13	13
N1A (bare soil)	0	0	0	0
N2 (seedling)	10	23	23	23
N3 (barren)	21	39	0	0
N4 (barren)	55	86	0	0
N5 (seedling)	0	12	12	12
N6 (barren)	51	83	83	85
X (bare soil)	0	0	0	0

Table 5. Vegetation height measurement at the southern sub-plot field of the Xiaotangshan Experiment in 2004 (units: cm).

Plot	h (25 June–7 July)
A (bare soil)	0
B, D (corn, medium height)	66.5
C (corn, low height)	37.2
E (corn, high height)	127.9
F (bare soil)	0
G (corn, high height)	104.2

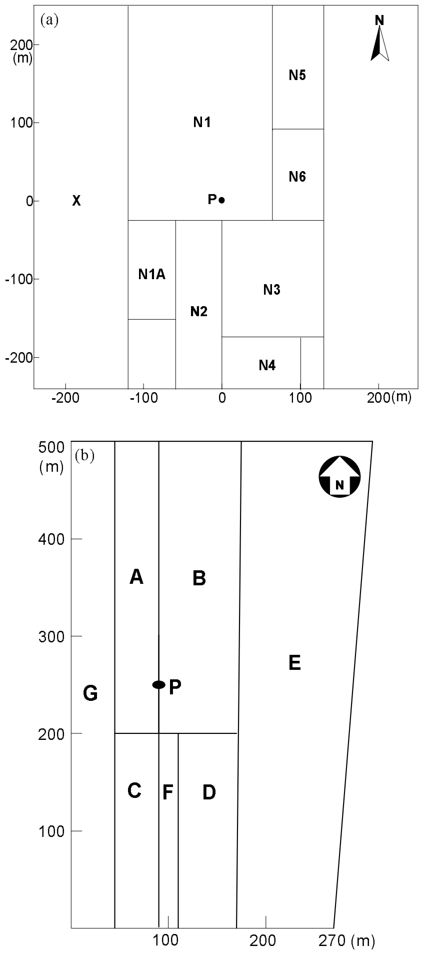

Fig. 2. The scheme of land cover over the Xiaotangshan experiment field. (P is the apparatus location; (a) northern sub-plot, N1: Morning glory field; N1A: bare soil; N2: seedling; N3: barren; N4: barren; N5: seedling; N6: barren; X: bare soil; (b) southern sub-plot, A, F: bare soil; B, D: corn, medium height; E, G: corn, high height; C: corn, low height)

and vegetation density varies. A standard value of 0.2 is generally recommended for $C_{\rm d}$ (Shaw and Pereira, 1982; Choudhury and Monteith, 1988).

The individual $z_{0\rm m}[z_{0\rm m}(i)$ for each surface component (patch)] of a heterogeneous surface can be estimated with Eq. (8). In former works, such as that by Taylor (1987), the aerodynamic roughness length for the whole area was aggregated from individual $z_{0\rm m}(i)$, with respective area as the weight:

$$\ln\langle z_{0\rm m}\rangle = \sum_i s_i \ln[z_{0\rm m}(i)] \ , \qquad (9)$$

where s_i represents the area ratio of patch i having roughness length $z_{0\rm m}(i)$ to the sum of all the patches. Angular brackets mean a spatial average. Since a footprint represents different contributions of individual patches in the source area and the effective roughness length should be the one that can produce a momentum to represent the spatial average of the surface stress occurring in the heterogeneous terrain, only the patches in the source area are considered. Furthermore, the respective footprint value of each patch is taken as the weight in the aggregation. Equation (9) can be corrected accordingly:

$$\ln\langle z_{0\rm m}\rangle = \sum_i p_i \ln[z_{0\rm m}(i)] \ , \qquad (10)$$

where $p_i = \sum f_{\rm patch}/\sum f_{\rm source\ area}$, with $\sum f_{\rm patch}$, $\sum f_{\rm source\ area}$ representing the sum of the footprint weight value in patch i and the whole source area respectively.

With Eqs. (8) and (9) or (8) and (10), the aerodynamic roughness length over heterogeneous surfaces, $\langle z_{0\rm m}\rangle$, can be calculated. Here, $\langle z_{0\rm m}\rangle$ is calculated for four wind directions mentioned above and the results are listed in Table 6. The corresponding $z_{0\rm m}$ measured by the eddy covariance system is also listed and treated as a reference value.

Compared with Eq. (9), $\langle z_{0\rm m}\rangle$ calculated by Eq. (10) is more agreeable with the reference value. The RMSD (root mean square difference) and MAPD (mean absolute percent difference) of the estimated $\langle z_{0\rm m}\rangle$ by Eqs. (9) and (10) compared with the reference value are 1.97 cm, 1.69 cm, and 64.2%, 57.4% respectively (Table 7). Apparently, footprint weighting is better than the area weighting in the aggregation process. This is expectable since the contribution of each patch in the source area to the sensor observation is different. Furthermore, since the footprint varies with aerodynamic factors (wind speed, wind direction, stability, etc.), the footprint weighting method can reflect the impact of those factors on $\langle z_{0\rm m}\rangle$.

Wang and Wang (1999) investigated the effective $z_{0\rm m}$ at a grid scale of a land surface scheme and supposed it was determined by the feature of each patch and its cover fraction, and considered the two respectively by means of assigning different weighting factors and adding them together. Following this idea,

Table 6. Overview of $z_{0\text{m}}$ calculated by Eqs. (9), (10), and (11) over heterogeneous surfaces. (units: cm)

Area	Wind direction	Measured $z_{0\text{m}}$	$z_{0\text{m}}$ [Eq. (9)]	$z_{0\text{m}}$ [Eq. (10)]	$z_{0\text{m}}$ [Eq. (11)] $a=b=1$	$z_{0\text{m}}$ [Eq. (11)] $a=2,b=1$	$z_{0\text{m}}$ [Eq. (11)] $a=4,b=1/4$
A (25 June–7 July 2004)	E	3.94	8.72	7.47	2.39	3.08	3.92
	S	4.30	4.62	6.63	2.32	2.90	3.48
	W	1.71	3.20	1.38	1.61	1.71	1.45
	N	1.34	3.43	3.31	1.91	2.21	2.31
B (21–31 May 2005)	E	1.88	2.51	1.90	1.60	1.76	1.75
	S	1.95	2.09	1.98	1.60	1.78	1.81
	W	0.95	1.28	1.47	1.46	1.56	1.48
	N	0.71	1.71	1.62	1.48	1.62	1.63

Table 7. The comparison between $z_{0\text{m}}$ calculated by Eqs. (9), (10), and (11) and the one estimated by measurements over heterogeneous surfaces.

Statistical parameters	$z_{0\text{m}}$ [Eq. (9)]	$z_{0\text{m}}$ [Eq. (10)]	$z_{0\text{m}}$ [Eq. (11)] $a=b=1$	$z_{0\text{m}}$ [Eq. (11)] $a=2,b=1$	$z_{0\text{m}}$ [Eq. (11)] $a=4,b=1/4$
RMSD (cm)	1.97	1.69	0.98	0.77	0.60
MAPD (%)	64.2	57.4	36.4	29.4	22.5

Figs. 3a and 3b are the scatter plots between the reference $z_{0\text{m}}$ and $\sum_i p_i \times (1/100)h(i)$ (where 1/100 is for matching to the order of measured $z_{0\text{m}}$), and $z_{0\text{m}}$ and $\sum_i p_i \times \text{LAI}(i)^{0.5}$ respectively. They all have obvious linear relations and the determination of the coefficient R^2 is 0.769 and 0.80, respectively. Further, the scatter plots between reference $z_{0\text{m}}$ and $\sum_i [p_i \times (1/100)h(i) + p_i \times \text{LAI}(i)^{0.5}]$ and $z_{0\text{m}}$ and $\sum_i p_i \times (1/100)h(i) \times \text{LAI}(i)^{0.5}$, respectively are given in Figs. 3c, 3d. The linear relation is apparent and R^2 equals 0.793 and 0.745, respectively. This may imply that, vegetation height and LAI represent size and density of the vegetation canopy respectively, they all have a drag effect on air flow but it is independent and accumulative. Referring to Eqs. (8) and (10), a parameterization is constructed below:

$$\ln\langle z_{0m}\rangle = \sum_i p_i \times \ln[z_0' + a \times \frac{1}{100}h(i) + b \times \text{LAI}(i)^{0.5}]\,, \qquad (11)$$

where a, b are constants and taken as weighting factors. Here three cases are discussed: (1) $a=b=1$; (2) $a=2, b=1$; (3) $a=4, b=1/4$. As before, $\langle z_{0\text{m}}\rangle$ can be calculated with the data of Group A and B using Eq. (11) and compared with the reference value (Tables 6, 7). Apparently, the results of Eq. (11) have a significant improvement compared with Eq. (10). Furthermore, the contribution of h and LAI on $\langle z_{0\text{m}}\rangle$ is different, the former is much more important than the latter, with the smallest RMSD and MAPD (0.60 cm and 22.5% respectively, Table 7) when the difference between a and b is the largest ($a=4, b=1/4$). This is expectable since the vegetation height has a predominant impact on $z_{0\text{m}}$. Sozzi et al. (1998) pointed out that "Even though $z_{0\text{m}}$ is not exactly equal to the height of roughness found on the earth's surface and encountered in the air masses' flow, a bi-univocal relation does exist between the two."

In addition, the linear relation between the reference z_{0m} and $\sum_i p_i \times f_v(i)^{0.5}$ (Fig. 3e) are also obvious, when R^2=0.817, which is a little higher than that of LAI (0.8). The same trend is found between the reference $z_{0\text{m}}$ and $\sum_i [p_i \times (1/100)h(i) + p_i \times f_v(i)^{0.5}]$ (Fig. 3f) with R^2 of 0.791, close to the one of LAI (0.793).

Based on the above analysis, a heuristic parameterization to calculate the aerodynamic roughness length, z_{0m}, over a heterogeneous surface is proposed:

$$\ln\langle z_{0\text{m}}\rangle = \sum_i p_i \times \ln\left[z_0' + a \times \frac{1}{100}h(i) + b \times V_e(i)^{0.5}\right]\,, \qquad (12)$$

where V_e is the characteristic factor of the roughness elements (leaf area index, or fractional vegetation cover). a and b are constants and can be seen as weighting factors and $a > b$. In this parameterization, the individual $z_{0\text{m}}$ of each homogeneous patch is calculated with the characteristic factors of the roughness elements, then aggregated to $\langle z_{0\text{m}}\rangle$ over a heteroge-

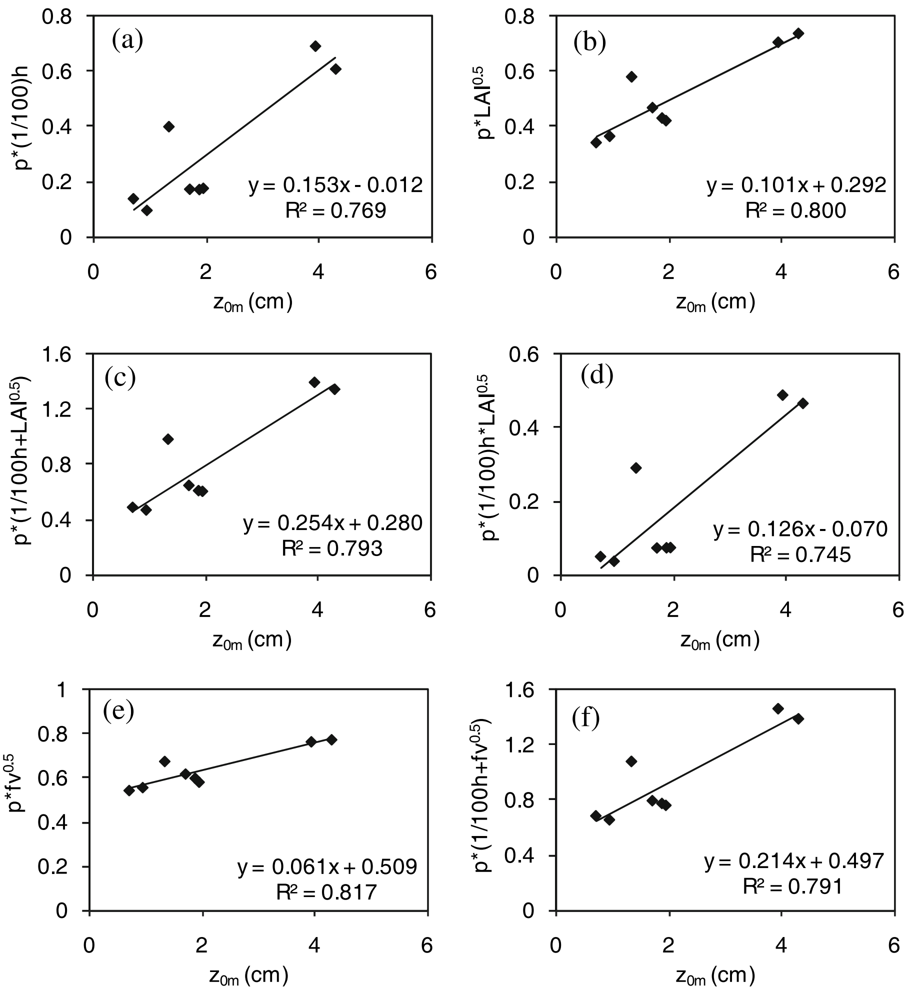

Fig. 3. The scatter plots between $z_{0\mathrm{m}}$ calculated with the sonic anemometer observational data and characteristic factors of the roughness elements.

neous surface by the footprint weighting method.

5. Summary and conclusions

This paper calculates $z_{0\mathrm{m}}$ over three different surfaces with data from the Xiaotangshan Experiment in 2002, 2004, and 2005. The order of $z_{0\mathrm{m}}$ is 0.1–1 cm. The value of $z_{0\mathrm{m}}$ varies with the variation of the roughness element height. According to the calculated $z_{0\mathrm{m}}$ at different wind directions, $z_{0\mathrm{m}}$ is direction-dependent. Over heterogeneous surfaces, the size and distribution of the roughness elements inside the source area are heterogeneous at different wind directions. Consequently, the $z_{0\mathrm{m}}$ value varies with the wind direction.

In surface flux estimations with remote sensing algorithms and/or land surface models, $z_{0\mathrm{m}}$ over heterogeneous surfaces at regional scales is needed. The proposed parameterization of this study Eq. (12) considers the height and density distribution of the roughness elements in the source area and the contribution of aerodynamic factors. The individual $z_{0\mathrm{m}}$ for each patch area is calculated with the characteristic factors of the roughness elements first and then, aggregated to $\langle z_{0\mathrm{m}}\rangle$ over heterogeneous surfaces by the footprint weighting method. This parameterization considers both the effect of the roughness elements and other meteorological conditions and is much simpler than the analogous parameterization by Massman (1997). The new parameterization is suitable for remote sensing model parameterizations at a regional scale. The constants a and b in Eq. (12) specify the different importance of the vegetation height and other factors to $\langle z_{0\mathrm{m}}\rangle$. More data is needed for further discussions.

Acknowledgements. This work was supported by the Hi-tech Research and Development Program of China (2007AA12Z175), the Special Research Foundation of the

Public Benefit Industry (GYHY200706046), the Project funded by the National Natural Science Foundation of China (Grant No. 40671128), and the National Basic Research Program of China (2007CB714401).

REFERENCES

Azevedo, P. V., and S. B. Verma, 1986: Aerodynamic characteristics of grain sorghum. *Agricultural and Forestry Meteorology*, **38**, 193–204.

Brutsaert, W., 1982: *Evaporation into the Atmosphere, Theory, History, and Applications.* D. Reidel, Boston, MA., 299pp.

Businger, J. A., J. C. Wyngaard, Y. Izumi, and E. F. Bradley, 1971: Flux profile relationships in the atmospheric surface layer. *J. Atmos. Sci.*, **28**, 181–189.

Cai, X., and M. Y. Leclerc, 2007: Forward-in-time and backward-in-time dispersion in the convective boundary layer: The concentration footprint. *Bound.-Layer Meteor.*, **123**, 201–218.

Chen, J., J. Wang, and Y. Mitsuta, 1993: An independent method to determine the surface roughness length. *Chinese J. Atmos. Sci.*, **17**(1), 21–26. (in Chinese)

Choudhury, B. J., and J. L. Monteith, 1988: A four-layer model for the heat budget of homogeneous land surfaces. *Quart. J. Roy. Meteor. Soc.*, **11**, 373–398.

Dai, Y., and Coauthors, 2003: The common land model (CLM). *Bull. Amer. Meteor. Soc.*, **84**(8), 1013–1023.

Dickinson, R. E., A. Henderson-sellers, and P. J. Kennedy, 1993: Biosphere-Atmosphere Transfer Scheme (BATS) Version 1e as coupled to the NCAR Community Climate Model. National Center for Atmospheric Research (NCAR) Tech. Note, NCAR/TN-387+STR, 72pp.

Dorman, J. L., and P. J. Sellers, 1989: A global climatology of albedo, roughness length, and stomatal resistance for atmospheric general circulation models as represented by the Simple Biosphere Model (SiB). *J. Appl. Meteor.*, **21**, 833–855.

Fiedler, F., and H. A. Panofsky, 1972: The geostrophic drag coefficient and the "effective" roughness length. *Quart. J. Roy. Meteor. Soc.*, **98**, 213–221.

Garratt, J. R., 1992: The atmospheric boundary layer. *Cambridge Atmospheric and Space Science Series*, Cambridge University Press, Cambridge, UK, 316pp.

Hatfield, J. L., 1989: Aerodynamic properties of partial canopies. *Agricultural and Forestry Meteorology*, **46**, 15–22.

Hiyama, T., M. Sugita, and K. Kotoda, 1996: Regional roughness parameters and momentum fluxes over a complex area. *J. Appl. Meteor.*, **35**, 2179–2190.

Jennifer, M., and W. Brusaert, 1998: Momentum roughness and view-angle dependent heat roughness at a Southern Great Plains test-site. *J. Hydrol.*, **211**, 61–68.

Jia, L., and J. Wang, 1999: The local and effective aerodynamic roughness length of a complex landscape of oasis and desert. *Acta Meteorologica Sinica*, **57**(3), 346–357. (in Chinese)

Jia, L., and Coauthors, 2003: Estimation of sensible heat flux using the Surface Energy Balance System (SEBS) and ATSR measurements. *Physics and Chemistry of the Earth*, **28**, 75–88.

Kormann, R., and F. X. Meixner, 2001: An analytical footprint model for non-neutral stratification. *Bound.-Layer Meteor.*, **99**, 207–224.

Kustas, W. P., B. J. Choudhury, K. E. Kunkel, and L. W. Gay, 1989: Estimate of the aerodynamic roughness parameters over an incomplete canopy cover of cotton. *Agricultural and Forestry Meteorology*, **46**, 91–105.

Liu, S., L. Lu, D. Mao, and L. Jia, 2007a: Evaluating parameterizations of aerodynamic resistance to heat transfer using field measurements. *Hydrology and Earth System Sciences*, **11**(2), 769–783.

Liu, S., G. Hu, L. Lu, and D. Mao, 2007b: Estimation of regional evapotranspiration by TM/ETM+ data over heterogeneous surfaces. *Photogrammetric Engineering and Remote Sensing*, **73**(10), 1169–1178.

Massman, W., 1997: An analytical one-dimensional model of momentum transfer by vegetation of arbitrary structure. *Bound.-Layer Meteor.*, **83**, 407–421.

Mason, P. J., 1988: The formation of areally averaged roughness lengths. *Quart. J. Roy. Meteor. Soc.*, **114**, 399–420.

Marshall, J. K., 1971: Drag measurement in roughness arrays of varying density and distribution. *Agricultural Meteorology*, **8**, 269–292.

Martano, P., 2000: Estimation of surface roughness length and displacement height from single-level sonic anemometer data. *J. Appl. Meteor.*, **39**, 708–715.

Mathias, A. D., W. P. Kustas, L. W. Gay, D. I. Cooper, L. M. Alves, and P. J. Pinter, 1990: Aerodynamic parameters for a sparsely roughened surface composed of small cotton plants and ridged soil. *Remote Sens. Environ.*, **32**, 143–153.

Menenti, M., and J. C. Ritchie, 1994: Estimation of effective aerodynamic roughness of Walnut Gulch watershed with laser altimeter measurements. *Water Resources Research*, **30**(5), 1329–1337.

Paulson, C. A., 1970: The mathematical representation of wind speed and temperature profiles in the unstable atmospheric surface layer. *J. Appl. Meteor.*, **9**, 857–861.

Schmid, H. P., 2002: Footprint modeling for vegetation and atmosphere exchange studies: a review and perspective. *Agricultural and Forest Meteorology*, **113**, 159–183.

Schuepp, P. H., M. Y. Leclerc, J. I. Macpherson, and R. L. Desjardins, 1990: Footprint prediction of scalar fluxes from analytical solutions of the diffusion equation. *Bound.-Layer Meteor.*, **50**, 355–373.

Shaw, R. H., and A. R. Pereira, 1982: Aerodynamic roughness of a plant canopy: a numerical experiment. *Agricultural Meteorology*, **26**, 51–65.

Sheng, P., J. Mao, J. Li, A. Zhang, J. Sang, and N. Pan, 2003: *Atmospheric Physics.* Peking University Press, Beijing, 522pp. (in Chinese)

Sozzi, R., M. Favaron, and T. Georgiadis, 1998: Method for estimation of surface roughness and similarity function of wind speed vertical profile. *J. Appl. Meteor.*, **37**, 461–469.

Taylor, P. A., 1987: Comments and further analysis on effective roughness lengths for use in numerical three-dimensional models. *Bound.-Layer Meteor.*, **39**, 403–418.

Wang, H., and X. Wang, 1999: *The Principles and Algorithm of Biological Boundary Layer*. Meteorology Press, Beijing, 211pp. (in Chinese)

Waters, R., R. Allen, W. Bastiaanssen, M. Tasumi, and R. Trezza, 2002: Surface energy balance algorithms for land, Idaho implementation, advanced training and users manual. Version 1.0, The Idaho Department of Water Resources, 98pp.

Webb, E. K., 1970: Profile relationships: The log-linear range and extension to strong stability. *Quart. J. Roy. Meteor. Soc.*, **96**, 67–90.

Wieringa, J., 1986: Roughness-dependent geographical interpolation of surface wind speed averages. *Quart. Roy. Meteor. Soc.*, **112**, 867–889.

Yang, K., T. Koike, and D. Yang, 2003: Surface flux parameterization in the Tibetan Plateau. *Bound.-Layer Meteor.*, **116**, 245–262.